

A New Decomposition to Interpret Curves of Schlumberger Survey

Mehran Azimbagirad, Arash Amiriam and Mohsen Oveisi Moakhar
Faculty of Sciences, Razi University, Kermanshah, Iran

Abstract: In this study, QR decomposition is utilized for 1D interpretation of Schlumberger sounding data instead of former method to optimize the best fit between the calculated and observed apparent resistivity data. The method is implemented by arbitrary parameters of initial model and uses the damped least-square solution with QR and LU decomposition. The method was tested on three synthetic models comparing with the Singular Value Decomposition (SVD) applicability. Noise also was added to two models. Furthermore, the procedure is employed to interpret real data from Iran and the results are compared with published previous geological information. In all cases, QR and LU Decompositions are quicker than SVD method to determine parameters of models.

Key words: Inversion methods, Schlumberger sounding, SVD, QR, LU decomposition

INTRODUCTION

Electrical detection includes the direction of surface effects produced by electric current flow beneath the earth surface. There are various techniques available than in the other detecting procedures where one use single field of force or anomalous property such as gravitation, magnetism, elasticity, radioactivity. By employing electrical methods, one can measure potentials, currents and electromagnetic fields that take place naturally or introduced artificially into the earth. In addition, the measurements can be made in different ways to reach different results. Principally, it is the enormous variation in electrical resistivity found in different rocks and minerals that makes these techniques possible.

All types of resistivity methods use a synthetic current source which is introduced into the earth through point electrodes or long line contacts; the latter arrangement is infrequently used nowadays. The method is for measuring potentials at other electrodes around the current flow. Because the current is measured as well. It is possible to find an effective or apparent resistivity of the geological structures in the ground. In this regard the resistivity technique is prior theoretically to other electrical procedures because quantitative results are obtained by using a controlled source of particular dimensions. In practice, the maximum potentialities of resistivity are never recognized. The tough difficulty is its high sensitivity to small changes in conductivity near surface; in electronic parlance the noise level is high (Karchani *et al.*, 2015).

The explorations carried out by using DC resistivity sounding method can give good output in the places that

have horizontal layers with unsubstantial lateral variation. The method has been used widely on many geophysical exploration problems. The most advantageous surveys have been carried out in hydrogeological, geothermal, environmental and engineering applications (Batayneh *et al.*, 2001; Mota *et al.*, 2004; Agnesi *et al.*, 2005; Ozurlan and Sahin, 2006; Asfaham and Radwan, 2007; Bauer *et al.*, 2006; Park *et al.*, 2007).

The apparent resistivity data do not yield real resistivity values of the subsurface structures. So, to determine the real resistivity distribution of the subsurface, inversion of the calculated apparent resistivity data should be put into practice. DC resistivity inverse problem was scrutinized for the first time in the early 1930s. Over the last decade, depending on high technological development of computer controlled multi-electrode survey systems and the inversion software, much of the studies performed on DC resistivity method have chiefly focused on 2D and 3D data acquisition and interpretation procedures (Nassir *et al.*, 2000; Bauer *et al.*, 2006; Ekinici *et al.*, 2008). However, 1D techniques can be used to interpret data and may give good approximation of the earth subsurface if the investigation is carried out in areas with slightly sloping or flat lying ground and where the resistivity and thickness variations between the adjacent layers are not tangible.

In this study, we present a MATLAB inversion program that uses damped least-squares solution to interpret Schlumberger sounding curves. The reliability of the present program was tested on both noisy and noise-free synthetic data.

MATERIALS AND METHODS

Schlumberger array is widely used because is not a complicated electrode configuration. The equation that relates the apparent resistivity data and parameters of the layers is an integral expression. This equation is also used for a forward response for Schlumberger electrode array $\rho\alpha$ on a ground with homogeneous, isotropic and horizontal layers. This equation is formulated as follow (Koefoed, 1970):

$$P_{\alpha} = S^2 \int_0^{\infty} T(\lambda) J_1(\lambda S) \lambda d\lambda \tag{1}$$

Where:

- s = The half current electrode spacing
- J_1 = The first order Bessel function of the first kind
- λ = The variable of the integral

Also, $T(\lambda)$ the resistivity transform function is given by the iterative Eq. 2:

$$T(\lambda) = \frac{T_{i+1}(\lambda) + \rho_i \tanh(\lambda h_i)}{\left[1 + T_{i+1}(\lambda) \tanh \frac{\lambda h_i}{P_i} \right]}, \tag{2}$$

$i = n - 1, \dots, 1$

Where:

- n = The number of layers
- ρ_i and h_i = The resistivity and thickness of the i th layer, respectively

Recent formula is utilized to calculate the forward response for DC resistivity sounding data.

To update iteratively the model parameters, non-linear least-square inversion method is used and in each iteration it uses a correction vector which is the solution of a pack of normal equations. This kind of inversion is an ill-posed problem. So, a small variation in the input data leads to a big variation in the model. Also, by optimizing we can restrict the rudimentary model to be near the true model. The complexity can be reduced by using damping into the set of equations (Roy, 1999). To reduce the DC level of eigenvalues one can add the parameters to the principal diagonal of AA^T (Raju, 2003). The damped least-squares is as follow (Levenberg, 1944):

$$\Delta p = (AA^T + \epsilon^2 I)^{-1} A^T \Delta d \tag{3}$$

Where:

- Δp = The parameter correction vector
- $A^{\Delta d}$ = The data difference vector
- A = The Jacobian matrix
- I = The identity matrix
- ϵ = Damping factor

SVD decomposition: Singular Value Decomposition(SVD) is common technique used in many areas of applied sciences including the earth sciences. According to Ekinci and Demirci (2008), it was discussed that SVD can be easily utilized to small scale geophysical problems. It is mathematically robust and numerically stable and also provides other vital information on the state of the model and data thus enabling model resolution and covariance studies (Meju, 1994). However, it must be noted that the use of SVD is not logical for large scale problems. Furthermore, it may has not more precise than others that we will mention it in next section. The large scale problems can be solved by other decompositions or iterative methods. A $n \times n$ or $n \times p$ matrix A can be factored into a product of three other matrices as follows:

$$A = USV^T \tag{4}$$

Where for n data and p parameters, U ($n \times p$) and V ($p \times p$) are respectively the data space and parameter space eigenvectors and S is a $p \times p$ diagonal matrix containing at most r non-zero eigenvalues of A with $r \leq p$. Suppose that members on main diagonal of S are presented by $(\lambda_1, \lambda_2, \dots, \lambda_p)$ which called singular values of A. This factorization is known as SVD of A (Meju, 1994). If SVD is used in damped least-squares solution, Eq. 4 is obtained:

$$\Delta p = (VS^2V^T + \epsilon^2 I)^{-1} VSU^T \Delta d \tag{5}$$

By adding the damping factor to the diagonal elements we obtain:

$$(VS^2V^T + \epsilon^2 I) = V \text{diag}(\lambda_j^2 + \epsilon^2) V^T \tag{6}$$

By inverting the Eq. 6 and substituting it in Eq. 5 is given by as follows:

$$\Delta p = V \text{diag} \left(\frac{1}{\lambda_j^2 + \epsilon^2} \right) V^T VSU^T \Delta d \tag{7}$$

And the parameter correction vector after simplification can be expressed as:

$$\Delta p = V \text{diag} \left(\frac{\lambda_j}{\lambda_j^2 + \epsilon^2} \right) U^T \Delta d \tag{8}$$

Equation 8 provides damped least-squares solution with SVD for automated inversion, the common practice is to set the damping factor first to a large positive value. Thus, taking the advantage of the good initial convergence properties of the steepest descent method and thereafter the damping factor is multiplied by a factor

smaller than unity after each iteration so that the least-squares method predominates near the solution (Meju, 1994). A way of determining the damping factor has been developed by (Arnason and Hersir, 1988) and given by as follows:

$$\varepsilon = \lambda_L \Delta X \frac{1}{L} \tag{9}$$

Where:

L = The test number performed for the damping factor at any iteration

h = The parameter eigenvalue

And the term of is given by:

$$\Delta X_r = \frac{X_{r-1} - X_r}{X_{r-1}} \tag{10}$$

Where:

x = The misfit value obtained in previous iteration

x = The misfit value of the current iteration

In this study, Eq. 9 and 10 were used to set the damping factor at each iteration.

QR and LU decomposition: The most powerful method to find eigenvalues of a symmetric tridiagonal matrix is QR algorithm. Given a symmetric tridiagonal matrix A, we factorize it as A = QR where the matrix Q is orthogonal (Q⁻¹ = Q^t) and R is an upper triangular matrix. We then reverse the order of the factors and obtain a new matrix B = RQ. If we repeat this process we obtain rapid convergence to a matrix which is diagonal, except that there may be 2×2 submatrices on the diagonal. The eigenvalues of A are then simply the eigenvalues of those 2×2 submatrices together with the values of the remaining elements on the diagonal. (Thus, in the simplest case where there are no 2×2 submatrices, the eigenvalues of A are just the diagonal elements). Another factorization for matrix A is LU which uses two matrices L and U (lower triangular and upper triangular matrix respectively) to represent A like:

$$A = LU \tag{11}$$

Then in order to solve system of equations Ax = b, it is enough to solve this problem in two stage:

$$Lz = b \text{ solve for } z, Ux = z \text{ solve for } x$$

It was indicated that solving these two systems is simple. QR and LU factorizations are implemented by MATLAB. We use both for comparing results encounter with former decomposition SVD. Final note that we should not forget is that in all kind of decomposition, the same damping factor is used.

RESULTS AND DISCUSSION

Synthetic examples: Synthetic models with ideal resistivity distributions of geological relevance were used in the applications. Three different examples consisting of three-or four-layered earth models were preferred. In general as a similar explanation mentioned by (Muiuane and Pedersen, 1999), the subsurface models where resistivity increases or decreases with depth are not difficult to resolve. On the other hand, if a resistor layer is embedded between two conductor layers or a conductor layer is embedded between two resistor layers, convergence is more difficult and slow in comparison to first type. We used these types of models for the numerical examples. The synthetic data were generated at a predetermined set of 20 AB/2 values for all models by using of the forward modeling function of the program. The 5% noise level is reasonable for sites with high resistivity contrasts and higher electrode contact resistances (Dahlin, 2001). Thus, models 2 and 3 were contaminated with +5% random noise depending on the magnitude of each data point.

Like (Ekinici and Demirci, 2008) we used homogeneous half spaces for the initial models. The inversion procedure was controlled by two misfit functions in the iteration. When the predetermined error limit was reached the inversion procedure was stopped automatically. The convergences were calculated as an rms error function between the observed and calculated apparent resistivity values at the end of the process as follows:

$$rms = \frac{\left(\sum_{i=1}^{ND} (d^{obs} - d^{cal})^2 \right)^{\frac{1}{2}}}{(ND)^{\frac{1}{2}}} \tag{12}$$

Where obs stands for observed and cal stands for calculated apparent resistivity values and ND stands for the number of the apparent resistivity data. The inversion results are illustrated as best-fit curves and resistivity-depth distributions for model 1-3 in following.

Model 1: First example demonstrates a noise-free three-layered earth model with decreasing resistivity with depth. In Table 1, although the amounts of errors are equal, the numbers of iterations shows that which method

Table 1: Observed and calculated apparent resistivity data of the model 1

Methods	SVD	LU	QR
Real values	Calculated	Calculated	Calculated
ρ1 = 100	Ωmp ₁ = 99.97	ρ1 = 99.97	ρ1 = 99.97
ρ2 = 50	Ωmp ₂ = 50.09	ρ2 = 50.09	ρ2 = 50.11
ρ3 = 20	Ωmp ₃ = 19.97	ρ3 = 19.97	ρ3 = 19.97
d ₁ = 5	md ₁ = 8.33	d ₁ = 8.33	d ₁ = 8.33

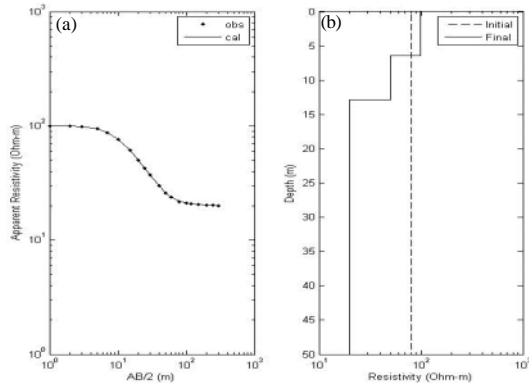


Fig. 1: Model 1, observed and calculated apparent resistivity curves

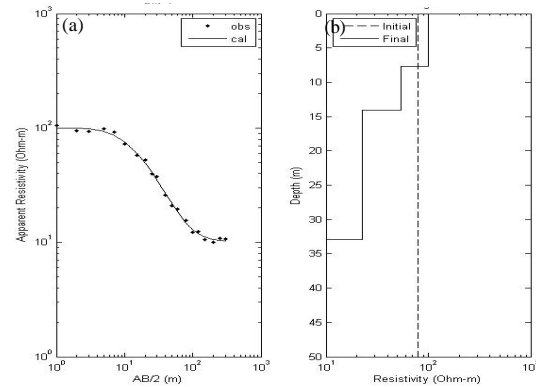


Fig. 3: Model 3, observed and calculated apparent resistivity curves

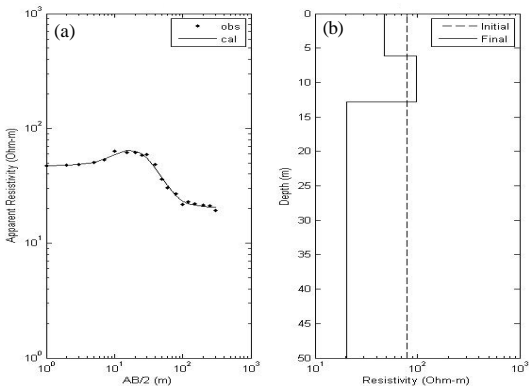


Fig. 2: Model 2, observed and calculated apparent resistivity curves

is the best. Left graph has two figures: observed and calculated apparent resistivity curves (Fig. 1) and resistivity-depth distribution of the initial and final models (Fig. 2). It is obvious that observed data are coincided with calculated in (Fig. 1). In (Fig. 2) we can see although the initial guesses were far removed from the true ones, the model parameters were resolved and the program yielded satisfactory results.

Model 2: Second example deals with a three-layered earth model consisting of a resistor layer between two conductors. Like Table 1 and 2 presents the best method in speed not in exactness because errors in all three methods are same.

Model 3: A four-layered decreasing resistivity with depth model was used in this example (Fig. 3). Like Table 1-3 presents the best method in speed not in exactness because errors in all three methods are same.

Table 2: Observed and calculated apparent resistivity data of the model 2

Methods	SVD	LU	QR
Real values	Calculated	Calculated	Calculated
$\rho_1 = 50$	$\Omega_{mp_1} = 47.40$	$\rho_1 = 47.40$	$\rho_1 = 47.40$
$\rho_2 = 100$	$\Omega_{mp_2} = 99.13$	$\rho_2 = 99.14$	$\rho_2 = 99.12$
$\rho_3 = 20$	$\Omega_{mp_3} = 20.35$	$\rho_3 = 20.35$	$\rho_3 = 20.35$
$d_1 = 5$	$md_1 = 7.95$	$d_1 = 7.95$	$d_1 = 7.95$

Table 3: Observed and calculated apparent resistivity data of the model 3

Methods	SVD	LU	QR
Real values	Calculated	Calculated	Calculated
$\rho_1 = 100$	$\Omega_{mp_1} = 99.89$	$\rho_1 = 99.87$	$\rho_1 = 99.83$
$\rho_2 = 50$	$\Omega_{mp_2} = 54.14$	$\rho_2 = 53.97$	$\rho_2 = 52.98$

Real data example: Harsin sheet is located in the Zagros Orogen zone and consists of various lithologic units of Sanandaj-Sirjan folds and over thrust. The majority of these units is allochthonous and is facially different from adjacent structures. Figure 1 and 2 show a part of the 1/100000 Harsin sheet. The highest point in this area is the Shiraz mount with 2700 height meters from the sea level. The lowest point is in the west of the Mal-Amiri village with 1287 height meters from the sea level. The average of rainfall is 600-1000 mm during the year. From the morphologic view, apart from lime altitudes, other parts of the area are covered by small hills. Rivers such as Gamasiab and Grezoo and also tectonic activity are significantly responsible for forming the altitudes and plains in the area of exploration. Water drainages in the area show the lineaments of faults. The alluvium consists of fine grained fluvial sediments, pebbles with 10 cm of diameter, limestone and Ophiolite. The average slope in the area is 5%. The locations of electric sounds are exactly on the alluvium. The Northern part of the area consists of crashed limestone. Faults in this formation likely have affected the alluvium. Also, Radiolarite accumulation is located in the North-East and South-East of the area.

The location of exploration area is at 3794412 Northern latitude and 741605 Eastern longitude in WGS84, UTM system. Thirty five sounds were implemented.

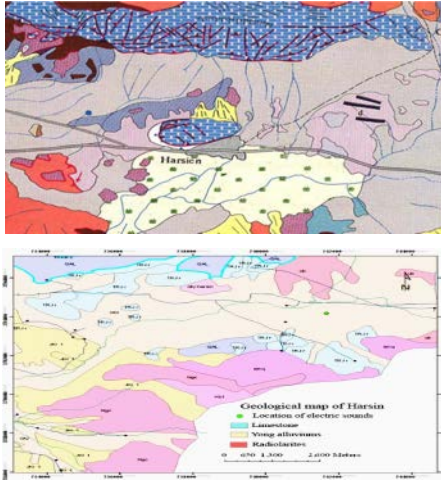


Fig. 4: The location map of area of exploration

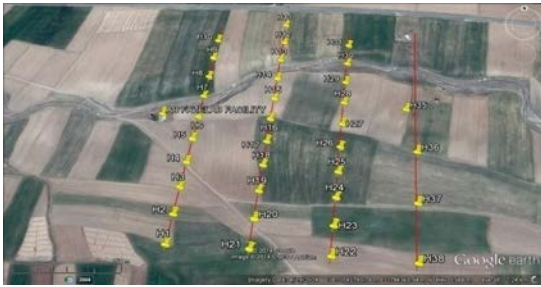


Fig. 5: The profiles of schlumberger soundings. Profiles have North-East direction

These sounds are on four profiles with North-South directions. The distance between two adjacent sounds is 50 m on profiles 1-3 and is 100 m on profile 4. Also, the distance between adjacent profiles is 100 m (Fig. 4). The data is collected by Schlumberger array. Figure 5 shows the profiles and sounds.

The geographical locations of sounds are given in Table 4. According to apparent resistivity data and Fig. 6 on this profile the value of apparent resistivity increases respect to the depth and reaches to 90 Ωm . Smooth changes in the amount of the apparent resistivity on this profile reveal that tectonic activity has not had significant impression on the characteristic of layers.

We chose H31 sounding curve on profile 3 to run the inversion programs and find the real amounts of resistivity at various depths and thicknesses of layers. Then, the results are compared with one another. We can see the results for recent data below (Fig. 7 and Table 5).

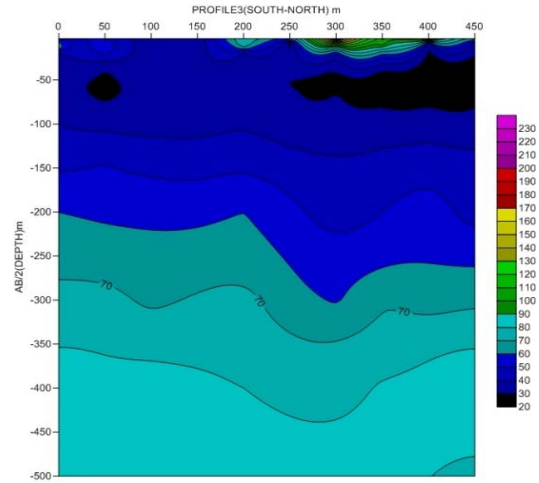


Fig. 6: Apparent resistivity of profile 3 V

Table 4: The longitude and latitude of every sounding

Sounds	Latitude	Longitude
Profile 1		
H1	3794157	741656
H2	3794208	741658
H3	3794257	741659
H4	3794306	741661
H5	3794356	741662
H6	3794406	741664
H7	3794456	741665
H8	3794506	741667
H9	3794556	741668
H10	3794605	741670
Profile 2		
H11	3794656	741795
H12	3794605	741795
H13	3794556	741791
H14	3794507	741789
H15	3794456	741787
H16	3794407	741784
H17	3794357	741782
H18	3794307	741780
H19	3794258	741778
H20	3794208	741776
H21	3794158	741774
Profile 3		
H22	3794154	741887
H23	3794204	741890
H24	3794254	741893
H25	3794304	741896
H26	3794353	741899
H27	3794403	741902
H28	3794453	741905
H29	3794503	741908
H30	3794552	741911
H31	3794602	741914
Profile 4		
H32	3794151	742005
H33	3794443	742008
H34	3794351	742019

Real model: It is worth to note that, in addition to the fact the number of iteration considerably has been decreased in our method, in this sounding curve interpretation; the error has been diminished as well though its amount may be tiny.

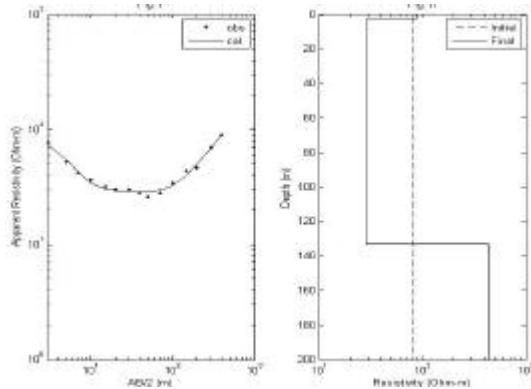


Fig. 7: Field example, observed and calculated apparent resistivity curves

Table 5: Observed and calculated apparent resistivity data of the fields example of model 4

Methods	SVD	QR
Real values	Calculated	Calculated
$\rho_1 = 87.33$	$\rho_1 = 87.63$	-
$\rho_2 = 28.10$	$\rho_2 = 28.12$	-

CONCLUSION

The present inversion scheme by using QR factorization is simple, fast and easy to carry out. The program uses damped least-squares solution with QR decomposition iteratively by updating the model parameters. The program was tested on small scale synthetically produced noise-free and noisy apparent resistivity data sets which have different curve types. Although, the initial guesses were far removed from the true ones, the present inversion program produced satisfactory results. Additionally, the results obtained by the inversion of the real data are in close agreement with the results of an earlier study. Finally we would like to explain this fact, nevertheless using QR decomposition and decreasing in number of iteration perhaps we have to have a lots of calculations (for QR level) time which is not good for new method. In final table we can see that CPU time (in a System with 3.2 GH speed with 4 Gigabyte RAM) in all models and two methods.

According to the results, the sounding curve indicates two alluvial layers. Shallow layer has a resistivity between 80-90 Ωm and a thickness of 2.5-3 m. This layer is mainly made of dry coarse drained alluvium (Fig. 8).

Second layer has a real resistivity of 20-3680 to 90 Ωm with a thickness of around 130-140 m. These show that this layer is also made of dry coarse drained alluvium and likely has water in middling and underneath parts. So the results are compatible with previous geological information.

CPU Time Comparison		
Methods:	SVD	QR
Models	CPU Time(s)	CPU Time(s)
Model 1	11.81	4.29

Fig. 8: A comparison between the time needed to calculate the parameters by SVD and QR methods

ACKNOWLEDGEMENTS

The researchers would like to express their gratitude to Dr. Sh. Heidarkhani for his precious advices to utilize proper mathematical methods. Also, we are grateful to H. Mousavi, the associate editor and two anonymous reviewers for their constructive suggestions and encouragement to improve the manuscript.

REFERENCES

Agnesi, V., M. Camarda, C. Conoscenti, C. Di Maggio, I.S. Diliberto, P. Madonia and E. Rotigliano, 2005. A multidisciplinary approach to the evaluation of the mechanism that triggered the Cerda landslide (Sicily, Italy). *Geomorphology*, 65: 101-116.

Arason, K. and G.P. Hersir, 1988. One dimensional inversion of Schlumberger resistivity soundings: Computer Program, Description and User's Guide: The United Nations University, Geothermal Training, Report 8, pp: 59.

Asfahani, J. and Y. Radwan, 2007. Tectonic evolution and hydrogeological characteristic of the Khanaser Valley, Northern Syria, derived from the interpretation of vertical electrical sounding. *P. Applied Geophys.*, 164: 2291-2311.

Batayneh, A.T., A.S. Al Zoubi and A.A. Abueladas, 2001. Geophysical investigations for the location of a proposed dam in Al Bishriyya (Al Aritayn) area, Northeast Badia of Jordan. *Environ. Geol.*, 40: 918-922.

Bauer, P., R. Supper, S. Zimmermann and W. Kinzelbach, 2006. Geoelectrical imaging of groundwater salinization in the Okavango Delta, Botswana. *J. Applied Geophys.*, 60: 126-141.

Dahlin, T., 2001. The development of DC resistivity imaging techniques. *Comput. Geosci.*, 27: 1019-1029.

- Ekinci, Y.L. and A. Demirci, 2008. A damped least-squares inversion program for the interpretation of schlumberger sounding curves. *J. Applied Sci.*, 8: 4070-4078.
- Ekinci, Y.L., A. Demirci and C. Ertekin, 2008. Delineation of the seawater-freshwater interface from the coastal alluvium of Kalekoy-Gokceada, NW Turkey. *J. Applied Sci.*, 8: 1977-1981.
- Karchani, M., A. Mazloumi, N.G. Saraji, A. Akbarzadeh and A. Niknezhad et al., 2015. Association of subjective and interpretive drowsiness with facial dynamic changes in simulator driving. *J. Res. Health Sci.*, 15: 250-255.
- Koefoed, O., 1970. A fast method for determining the layer distribution from the raised kernel function in geoelectrical soundings. *Geophys. Prospect.*, 18: 564-570.
- Levenberg, K., 1944. A method for the solution of certain non-linear problems in least-squares. *Q. Applied Math.*, 2: 164-168.
- Marquardt, D.W., 1963. An Algorithm for least-squares estimation of nonlinear parameters. *J. Soc. Ind. Applied Math.*, 11: 431-441.
- Meju, M.A., 1994. *Geophysical Data Analysis: Understanding Inverse Problem Theory and Practice*. Society of Exploration Geophysics Course Notes Series, No. 6, 1st Edn., SEG Publishers, Tulsa, Oklahoma, ISBN: 1-56080-027-5, pp: 296.
- Mota, R., F.A.M. Santos, A. Mateus, F.Q. Marques, M.A. Goncalves, J. Figueiras and H. Amaral, 2004. Granite fracturing and incipient pollution beneath a recent landfill facility as detected by geoelectrical surveys. *J. Applied Geophys.*, 57: 11-22.
- Muiwane, E.A. and L.B. Pedersen, 1999. Automatic 1D interpretation of DC resistivity sounding data. *J. Applied Geophys.*, 42: 35-45.
- Nassir, S.S.A., M.H. Loke, C.Y. Lee and M.N.M. Nawawi, 2000. Salt-water intrusion mapping by geoelectrical imaging surveys. *Geophys. Prospect.*, 48: 647-661.
- Ozurlan, G. and M.H. Sahin, 2006. Integrated geophysical investigations in the Hisar geothermal field, Demirci, Western Turkey. *Geothermics*, 35: 110-122.
- Park, Y.H., S.J. Doh and S.T. Yun, 2007. Geoelectric resistivity sounding of riverside alluvial aquifer in an agricultural area at Buyeo, Geum River watershed, Korea: An application to groundwater contamination study. *Environ. Geol.*, 53: 849-859.
- Raju, D.C.V., 2003. LIMAT: A computer program for least-squares inversion of magnetic anomalies over long tabular bodies. *Comput. Geosci.*, 29: 91-98.
- Roy, I.G., 1999. An efficient non-linear least-squares 1D inversion scheme for resistivity and IP sounding data. *Geophys. Prospect.*, 47: 527-550.